THE JOURNAL OF BIOLOGICAL CHEMISTRY VOL. 282, NO. 52, pp. 37836–37843, December 28, 2007

Identification of a Lysosomal Peptide Transport System Induced during Dendritic Cell Development*[S]

Received for publication, March 28, 2007, and in revised form, October 26, 2007 Published, JBC Papers in Press, October 31, 2007, DOI 10.1074/jbc.M708139200

Özlem Demirel[‡], Zoe Waibler[§], Ulrich Kalinke[§], Frank Grünebach[¶], Silke Appel[¶1], Peter Brossart[¶], Andrej Hasilik[‖], Robert Tampé[‡2], and Rupert Abele[‡3]

From the [‡]Institute of Biochemistry, Biocenter, Goethe-University Frankfurt, Max-von-Laue-Strasse 9, Frankfurt/M. D-60438, the [§]Division of Immunology, Paul-Ehrlich-Institut, Paul-Ehrlich-Strasse 51–59, Langen D-63225, the [¶]Department of Hematology, Oncology and Immunology, Eberhard-Karls-University Tübingen, Otfried-Müller-Strasse 10, Tübingen D-72076, and the [‖]Institute of Physiological Chemistry, Philipps-University Marburg, Karl-von-Frisch-Strasse 1, Marburg D-35032, Germany

The delivery of protein fragments to major histocompatibility complex (MHC)-loading compartments of professional antigen-presenting cells is essential in the adaptive immune response against pathogens. Apart from the crucial role of the transporter associated with antigen processing (TAP) for peptide loading of MHC class I molecules in the endoplasmic reticulum, TAP-independent translocation pathways have been proposed but not identified so far. Based on its overlapping substrate specificity with TAP, we herein investigated the ABC transporter ABCB9, also named TAP-like (TAPL). Remarkably, TAPL expression is strongly induced during differentiation of monocytes to dendritic cells and to macrophages. TAPL does not, however, restore MHC class I surface expression in TAP-deficient cells, demonstrating that TAPL alone or in combination with single TAP subunits does not form a functional transport complex required for peptide loading of MHC I in the endoplasmic reticulum. In fact, by using quantitative immunofluorescence and subcellular fractionation, TAPL was detected in the lysosomal compartment co-localizing with the lysosome-associated membrane protein LAMP-2. By *in vitro* assays, we demonstrate a TAPL-specific translocation of peptides into isolated lysosomes, which strictly requires ATP hydrolysis. These results suggest a mechanism by which antigenic peptides have access to the lysosomal compartment in professional antigen-presenting cells.

In the adaptive immune system, T-lymphocytes monitor the peptide repertoire presented in complex with major histocompatibility complex (MHC)[4] molecules on the cell surface to identify exogenous or endogenous pathogens. In the classical MHC class I-mediated immune response, TAP is an essential factor for transporting peptides, generated in the cytosol primarily by proteasomal degradation, into the ER lumen (1). These peptides bind to MHC class I and are shuttled in complex to the cell surface. Exogenous antigens are taken up via the endocytic pathway, and, after fragmentation in lysosomal compartments, peptides are loaded onto MHC class II (2). In professional antigen-presenting cells like macrophages, dendritic cells, and B-cells, a process termed cross-presentation exists, in which MHC class I presents exogenous antigens, whereas cytosolically generated peptides of endogenous origin are displayed by MHC class II on the cell surface (3, 4). In both cases, a TAP-independent pathway has been proposed but not yet identified (5–7).

Most recently, TAPL was uncovered as an ATP-dependent peptide transporter, sharing some degree of overlap in substrate specificity with TAP (8). TAPL transports a very broad spectrum of peptides ranging from 6- up to 59-mers (8), whereas TAP prefers peptides with a length of 8–12 amino acids (9). Both transporters belong to the superfamily of ABC proteins (10). Members of this family are found in all three phyla of life, where they translocate a very broad range of solutes across membranes. Functional complexes are built up either by heterodimers of TAP1 and TAP2, or homodimers of TAPL (8, 11–13). However, whether TAPL can assemble with TAP1 or TAP2 into a functional transport complex is still an open issue (14). TAPL and TAP share a similar exon organization and a high degree of sequence similarity (15–17). Because TAP is an essential factor in the MHC class I pathway, cells lacking TAP1 or TAP2 show a strongly impaired surface expression of MHC class I molecules (18, 19).

The involvement of TAP in antigen presentation is also mirrored by the localization of its genes in the MHC class II locus (20), whereas *tapl* is not clustered with genes relevant for the immune system (21). Based on phylogenetic analyses, TAPL appears to be the ancestral peptide transporter present even in

* This work is supported by Studienstiftung des Deutschen Volkes (to Ö. D.). The costs of publication of this article were defrayed in part by the payment of page charges. This article must therefore be hereby marked "*advertisement*" in accordance with 18 U.S.C. Section 1734 solely to indicate this fact.

[S] The on-line version of this article (available at http://www.jbc.org) contains supplemental Figs. S1–S3.

[1] To whom correspondence may be addressed: Tel.: 49-69-798-29475; Fax: 49-69-798-29495; E-mail: tampe@em.uni-frankfurt.de.

[2] To whom correspondence may be addressed: Tel.: 49-69-798-29437; Fax: 49-69-798-29495; E-mail: abele@em.uni-frankfurt.de.

[3] Present address: Broegelmann Research Lab., The Gade Inst., University of Bergen, N-5021 Bergen, Norway.

[4] The abbreviations used are: MHC, major histocompatibility complex; ABC, ATP-binding cassette; DC, dendritic cell; EEA1, early endosome antigen 1; ER, endoplasmic reticulum; LAMP, lysosome-associated membrane protein; LPS, lipopolysaccharides; NBD, nucleotide-binding domain; TAP, transporter associated with antigen processing; TAPL, transporter associated with antigen processing-like; TMD, transmembrane domain; TNF, tumor necrosis factor; PE, phycoerythrin; RT, reverse transcription; GAPDH, glyceraldehyde-3-phosphate dehydrogenase; EGFP, enhanced green fluorescent protein; GM-CSF, granulocyte/macrophage colony-stimulating factor; IL, interleukin; FACS, fluorescence-activated cell sorting.

jawless vertebrates lacking an adaptive immune system (17). In contrast to TAP, which is expressed in all somatic cells, TAPL is strongly expressed in testes, whereas moderate expression levels are found in brain, spinal cord, and heart (15, 22). The subcellular localization of TAPL is a matter of debate, because it was identified in lysosomes (15) as well as in the ER (14, 21).

In this study, we investigated the role of TAPL in the adaptive immune system. We observed a strong up-regulation of TAPL expression during maturation of dendritic cells and macrophages. By using quantitative immunofluorescence and subcellular fractionation, TAPL was found in the lysosomal compartment. In agreement with this, TAPL is not involved in the peptide delivery into the classical MHC class I loading compartment, because TAPL did not restore MHC class I cell surface expression of TAP-deficient cells. By establishing an *in vitro* assay, we demonstrated for the first time a TAPL-specific ATP-dependent translocation of peptides into isolated lysosomes. The identification of a new transport system in the lysosomal compartment as well as its strong up-regulation during maturation of DCs and macrophages suggest that TAPL is part of an alternative pathway of antigen presentation in professional antigen-presenting cells.

EXPERIMENTAL PROCEDURES

Cloning—Human TAPL was cloned into pEGFP-N3 and pIRES2-EGFP (both BD Biosciences) resulting in TAPL with a C-terminal EGFP and TAPL co-translated with EGFP, respectively. Furthermore, TAPL containing a C-terminal *myc* tag was cloned into pcDNA3.1(+) (Invitrogen). These constructs were PCR-amplified using the primer pairs pcDNA3.1(+)-TAPL-*myc* (5′-CGATTAGCTAGCATGCGGCTGTGGAAG-3′ and 5′-CGATTAGGATCCTCACAGATCCTCTTCTGAGATGAGTTTTTGTTCACTGCCGGCCTTGTGACTGCC-3′), pEGFP-N3-TAPL (5′-CGATTAGCTAGCATGCGGCTGTGGAAGG-3′ and 5′-CGATTAGGATCCGGCCTTGTGACTGCC-3′), and pIRES2-TAPL-EGFP (5′-CGATTAGCTAGCATGCGGCTGTGGAAGG-3′ and 5′-CGATTAGGATCCTCAGGCCTTGTGACTGCC-3′) and cloned via NheI and BamHI sites into the vectors. For cloning of TAPL into the retroviral vector pLPCX (Clontech), ClaI and BglII restriction sites were introduced by PCR via the primer pairs 5′-GAAGATCTTCGCCACCATGCGGCTGTGGAAGG-3′ and 5′-CCATCGATGGTCAGGCCTTGTGACTGCC-3′. TAPL-K545A/H699A was generated by Ligase Chain Reaction using the primers 5′-CGGGCAGTGGGGCGAGCTCCTGTGTC-3′ and 5′-CTCATCATCGCGGCCCGGCTGAGCAC-3′ (mutated bases are underlined). p46.TAP1wt DNA was used for transient expression of human TAP1 in BRE-169 cells (23).

Cell Lines and Culture—BRE-169 or STF1-169 cells are TAP1- or TAP2-deficient skin fibroblast cell lines, respectively (19). HeLa, BRE-169, STF1-169, and 293T cells were cultured in Dulbecco's modified Eagle's medium (PAA Laboratories) containing 10% fetal calf serum (Biochrom AG), 1 mM sodium pyruvate, 2 mM L-glutamine, 100 μg/ml penicillin, and 100 μg/ml streptomycin. For BRE-169 and STF1-169 cells, 50 μg/ml hygromycin was supplemented. For stably TAP2-transfected STF1-169 cells, 500 μg/ml neomycin was added to the medium (23). Human Burkitt lymphoma cells (Raji cells) were cultured as reported previously (24). THP-1 cells were grown in RPMI 1640 medium (PAA Laboratories) containing 10% fetal calf serum and were stimulated with *Escherichia coli* as described elsewhere (25).

Generation of DCs—DCs were generated in two different ways. In the first method, human peripheral blood monocytes were isolated by Ficoll density gradient centrifugation and monocytes isolated using anti-CD14 micro beads according to the manufacturer's instructions (Miltenyi Biotech). 1×10^6 monocytes per 24-well plate were cultured in DC medium (CellGro) supplemented with 1000 units/ml GM-CSF (Biomedical Laboratories) and 1000 units/ml IL-4 (Peprotech) for 5 days to obtain immature DCs. For differentiation into mature DCs, immature DCs were additionally stimulated from days 5 to 8 with a maturation mixture (26): 10 ng/ml IL-1β (Peprotech), 10 ng/ml TNF-α (Peprotech), 1000 units/ml IL-6 (Peprotech), and 1 μg/ml prostaglandin E_2 (Sigma). In the second method, monocyte-derived DCs were generated as described previously (27). To inhibit differentiation of monocytes, IL-10 (10 ng/ml, R&D Systems) was added together with GM-CSF and IL-4. The medium was replenished with cytokines every 2 or 3 days. For maturation, DCs were further cultured with additional stimuli as TNF-α (10 ng/ml, R&D Systems), lipopolysaccharides (LPS, 100 ng/ml, Sigma), Pam3Cys (5.0 μg/ml, EMC Microcollection), poly I:C (50.0 μg/ml, Sigma), R848 (2.0 μg/ml, InvivoGen), or CD40L (100 ng/ml, Bender Medsystem) for 24 h.

RT-PCR—RT-PCR was performed using two different protocols. With the first method, total RNA was prepared using TRIzol reagent (Invitrogen) according to the manufacturer's instructions. DNA was removed by treatment with DNase (Roche Applied Science) for 15 min at 37 °C, and cDNA was prepared by using SuperScript II (Invitrogen) according to the manufacturer's instructions. PCRs were performed using the following primer pairs: TAPL, 209 bp (5′-GCTCTGGGAGAGACCTTCCT-3′ and 5′-GAGCGGAAGAGACAGTTTCG-3′), TAPL, 538 bp (5′-CAAGTACTACAAGAGGCTCTCCAAAG-3′ and 5′-GGAGACATTCTGCAGGACCTG-3′), GAPDH (5′-ACCACAGTCCATGCCATCAC-3′ and 5′-TCCACCACCCTGTTGCTGTA-3′), and β_2-m (5′-GGGTTTCATCCATCCGACAT-3′ and 5′-GATGCTGCTTACATGTCTCGA-3′). The mRNA content was normalized by RT-PCR analysis with GAPDH-specific primers. PCRs using RNA before reverse transcription as template confirmed the absence of genomic DNA in the samples. With the second method, total RNA was isolated from cell lysates using Qiagen RNeasy Mini anion-exchange spin columns, including on-column DNase digestion (Qiagen), according to the instructions of the manufacturer. Total RNA (1 μg) was subjected to a 20.0-μl cDNA synthesis reaction (Transcriptor First Strand cDNA Synthesis Kit, Roche Applied Science) using random hexamer primers. 1.0 μl of cDNA was used for PCR amplification. To control the integrity of RNA and the efficiency of cDNA synthesis, 1.0 μl of cDNA was amplified by an intron-spanning primer pair for the β_2-microglobulin gene.

Transfection—BRE-169 and STF1-169 cells (2×10^6 cells) or HeLa cells (1×10^7 cells) were electroporated in 400 μl of electroporation buffer (20 mM HEPES, 137 mM NaCl, 5 mM KCl, 0.7

mM Na_2HPO_4, 6 mM dextrose, pH 7.05) in the presence of 6 μg or 30 μg DNA, respectively. Electroporation was performed with a GenePulser II (Bio-Rad, gene pulser cuvettes (0.4-cm electrode gap), 260 V, 350 microfarads, and 50 Ω). The cells were diluted in 10 ml of recovery medium (culture medium containing 3 mM EGTA) for 30 min at 37 °C. Cells were subsequently transferred to fresh culture medium.

Retroviral Transduction—Recombinant retroviruses were obtained by co-transfection of pCL-Ampho (generous gift of Peter Cresswell) (28), and the retroviral constructs pLPCX-TAPL or pLPCX-TAPL-K545A/H699A into 293T cells with Lipofectamine 2000 (Invitrogen) following the manufacturer's instructions. Supernatants were collected 30 h after transfection and filtered through a 0.45-μm pore size filter. For transduction, 1×10^6 Raji or THP-1 cells were resuspended in 2 ml of viral supernatant supplemented with 8 μg/ml Polybrene (Sigma). Cells were transferred into 6-well plates and centrifuged at 1250 $\times$ *g* for 90 min at 32 °C. After 15 h, cells were transferred to normal medium, and after recovery for 6–8 h, the transduction was repeated. 24 h after, cells were selected in medium containing 0.5 μg/ml puromycin (Sigma).

Flow Cytometry—BRE-169 and STF1-169 cells were harvested 48 h after electroporation, washed once in FACS buffer (phosphate-buffered saline, 2% fetal calf serum), and blocked with bovine serum albumin buffer (FACS buffer containing 5% bovine serum albumin). Afterward, 5×10^5 cells were stained with a phycoerythrin (PE)-conjugated anti-human HLA-ABC (W6/32, eBioscience) or PE-conjugated mouse IgG_2 isotype control antibody (eBioscience) and analyzed by flow cytometry with a FACSAria cell sorter (BD Biosciences) controlled by FACSDiVa software (BD Biosciences). Routinely, 30,000 cells were counted for one measurement. The data were analyzed with FCS-Express software (De Novo Software). Monocytes as well as immature and mature DCs were washed twice with phosphate-buffered saline and immunostained in the presence of polyglobin for 20 min at 4 °C using the following monoclonal antibodies diluted to the optimal concentration: anti-CD14-Pacific blue (BD Pharmingen), anti-HLA-DR-APC-Cy7 (Biolegend), anti-CD83-APC (BD Pharmingen), and anti-CD86-PE (Biolegend). Cells were analyzed by flow cytometry using LSR II with DIVA and/or WinList software.

Quantitative Immunofluorescence—Stably transduced and stimulated THP-1 cells or HeLa cells grown on poly-D-lysine-coated coverslips were fixed for 12 min at room temperature in 2% paraformaldehyde in phosphate-buffered saline and permeabilized with 0.1% Triton X-100 for 20 min at room temperature. After blocking with 5% bovine serum albumin, cells were stained with the primary antibody (rabbit anti-calnexin polyclonal antibody (Stressgen), mouse anti-calnexin (Dianova), rabbit anti-EEA1 polyclonal antibody (Calbiochem), mouse anti-EEA1 (Abcam), anti-*myc* monoclonal antibody (BD Biosciences), anti-LAMP-2 monoclonal antibody (2D5) (29), epitope-purified, rabbit anti-TAPL polyclonal antibody (8)) followed by fluorescence-labeled secondary antibody (Cy3 donkey anti-rabbit antibody, Cy3 donkey anti-mouse antibody, Alexa Fluor 488 goat anti-mouse antibody (Dianova)) for 30 min each at room temperature. Preparations were mounted in 0.1 M Tris/HCl, pH 8.5, 25% (w/v) glycerol, 10% (w/v) Mowiol (Calbiochem), and 2.5% 1,4-diazabicyclo[2.2.2.]octane (Sigma). Samples were analyzed with a confocal laser-scanning microscope (LSM 510, Zeiss) using the argon laser line at 488 nm for Alexa Fluor 488 or EGFP excitation and a 543 nm HeNe laser for excitation of Cy3. Fluorescence was detected through a 505–530 nm band pass filter and a 560 nm long pass filter for the argon laser and HeNe laser excitation, respectively. 512 $\times$ 512 pixels per image were recorded with a Plan-Apochromat 63$\times$ oil immersion objective (numerical aperture, 1.4). To reduce blur, improve resolution, and reduce background, blind deconvolution with the program Auto Deblur (Bitplane AG, Switzerland) was performed. The restored images were used for the co-localization analysis with the software package Imaris (Bitplane AG). The threshold was set to 50 to eliminate influence of background for co-localization. For each pair of co-localization analysis, the number of co-localized voxels was determined from 2 to 10 images.

Preparation of Lysosomes—2×10^8 Raji or stimulated THP-1 cells were harvested, washed once in HEPES buffer (10 mM HEPES, 1 mM EDTA, 250 mM sucrose, pH 7.4), and homogenized in a Dounce homogenizer. The homogenate was centrifuged at 1,000 $\times$ *g* for 5 min, and the post-nuclear supernatant was layered on 31% (v/v) Percoll underlayed with a cushion of 27.6% Nycodenz solution. The gradient was centrifuged at 40,000 $\times$ *g* for 1 h. 14 fractions were collected and analyzed by SDS-PAGE and immunoblotting using TAPL (8), LAMP-2 (29), and tapasin-specific antibodies (30). Fraction 14 corresponding to the dense pool of lysosomes was used for the peptide translocation assay.

Peptide Transport—In vitro transport assays were performed with the dense pool of lysosomes in the presence of 2 μM fluorescein-labeled peptide RRYC(Φ)KSTEL (Φ indicates fluorescein coupled via a cysteine residue) in a total volume of 150 μl of HEPES buffer containing 10 mM $MgCl_2$. For competition or inhibition, 500 μM non-labeled peptide or 1 mM orthovanadate was added, respectively. Transport was performed in the presence of ATP or AMP (3 mM) for 30 min at 32 °C. Thereafter, the transport was stopped with stop buffer (HEPES buffer with 10 mM EDTA and 50 μM non-labeled peptide RRYQKSTEL). After 15-min incubation on ice, samples were transferred to microfilter plates preincubated with 0.3% polyethyleneimine (MultiScreen plates, Durapore membrane, 1-μm pore size, Millipore). Filters were washed three times with 250 μl of ice-cold HEPES buffer containing 10 mM EDTA. Subsequently, the filters were incubated with 250 μl of elution buffer (phosphate-buffered saline, 1% SDS) for 10 min. Fluorescent peptides were quantified with a fluorescence plate reader (excitation and emission at 485 and 520 nm, respectively, BMG, Polarstar Galaxy).

RESULTS

TAPL Expression Is Strongly Induced during Differentiation of Monocytes to Dendritic Cells—On the transcriptional level, TAPL expression has been found in different tissues (15, 22). However, TAPL protein expression was shown only in Sertoli cells (15). Because the supply and cellular compartmentalization of antigenic peptides is of key importance for manifestation of an adaptive immune response, we examined TAPL

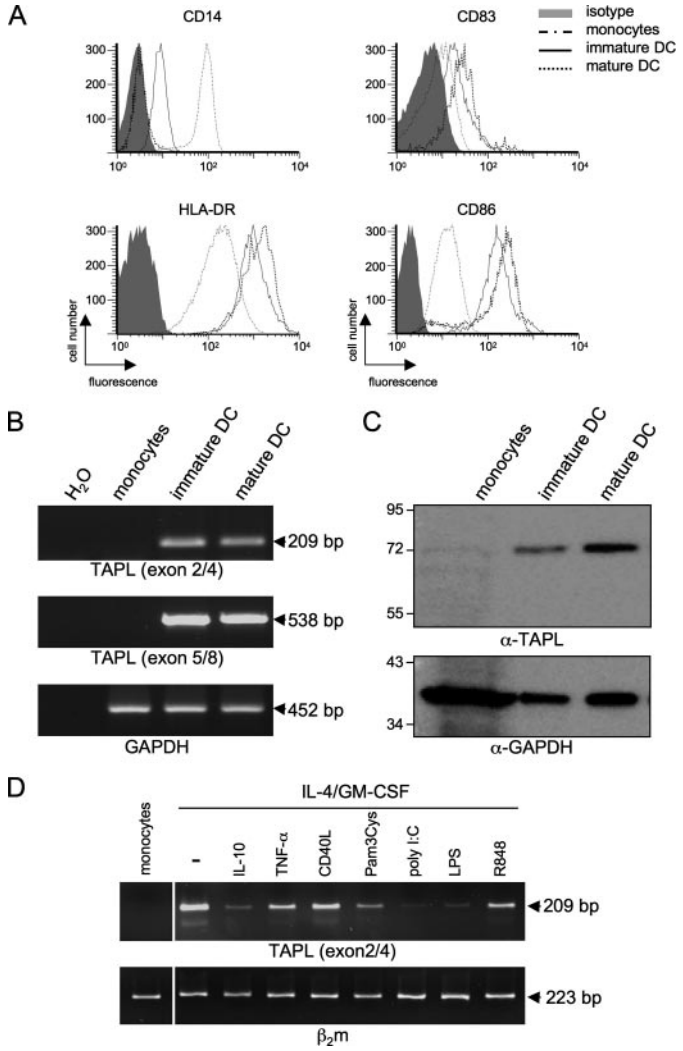

FIGURE 1. **TAPL expression in dendritic cells.** $CD14^+$ peripheral blood monocytes were isolated and stimulated by GM-CSF and IL-4 for 5 days to immature DCs. Further stimulation for 3 days by a maturation mixture (26) induced differentiation to mature DCs. *A*, maturation of DCs. The degree of maturation was detected by flow cytometry using antibodies against CD14, HLA-DR, CD83, and CD86. *B*, RT-PCR of monocytes as well as immature and mature DCs. Primer pairs specific for exon 2/4 or exon 5/8 were used. GAPDH mRNA serves as an internal control. *C*, immunodetection of monocytes as well as immature and mature DCs. Monocytes before and after stimulation were lysed, and proteins were separated by SDS-PAGE followed by immunoblotting. TAPL was detected using an epitope-purified TAPL-specific antibody. An equal amount of protein per lane was verified by anti-GAPDH staining. *D*, human peripheral blood monocytes were isolated and stimulated with GM-CSF and IL-4 for 6 days resulting in immature DCs or GM-CSF, IL-4, and IL-10 to inhibit differentiation. Mature DCs were derived by further stimulation for 24 h in the presence of additional stimuli as indicated. RT-PCR with a primer pair specific for exon 2/4 was performed. To verify equal amounts of mRNA, RT-PCR with β_2m-specific primers was performed.

expression in professional antigen-presenting cells. Human $CD14^+$ peripheral blood monocytes were isolated and cultured in medium containing GM-CSF and IL-4. After 5 days of incubation, monocytes differentiated to immature DCs as indicated by the loss of CD14 surface expression and the up-regulation of MHC class II, CD83 and CD86 on the cell surface (Fig. 1*A*). Incubation for further 3 days with a cytokine mixture containing IL-1β, TNF-α, IL-6, and prostaglandin E_2 (26) resulted in the maturation of DCs as indicated by further increase in MHC class II, CD83, and CD86 surface expression.

First, mRNA levels of TAPL were studied using primers binding to exons 2 and 4 of *tapl*, resulting in a PCR product of 209 bp (Fig. 1*B*). In monocytes, no mRNA for TAPL was detected by RT-PCR, whereas differentiation of monocytes with GM-CSF and IL-4 to immature DCs strongly increased the mRNA level of TAPL. Further maturation of DCs did not significantly change the transcriptional level of TAPL. RT-PCR analysis with primers binding to exons 5 and 8 gave similar results. Here, a single PCR product of 538 bp was detected for all donors analyzed, excluding the presence of the splice variant reported previously, lacking exon 7 (expected PCR product of 409 bp) (15).

The mRNA level may not necessarily reflect the expression level of TAPL. We therefore investigated TAPL expression on the protein level by immunoblotting using an antibody specific for the splice variant 12A of TAPL (Fig. 1*C*), which is active in ATP-dependent peptide transport (8). In monocytes isolated from various donors, TAPL expression was not detectable. However, after differentiation to immature and mature DCs, expression of TAPL was strongly induced. TAPL was detected as a single band at an apparent molecular mass of ~72 kDa. TAPL runs faster than the theoretical mass of 84 kDa. This behavior is typical for very hydrophobic proteins (8).

We next examined the regulation of TAPL mRNA levels upon stimulation of immature DCs in more detail (Fig. 1*D*). Monocytes treated with GM-CSF and IL-4 in combination with IL-10, which inhibits DC development (31–33), expressed very low amounts of TAPL mRNA. Furthermore, immature DCs stimulated by specific ligands, such as Pam3Cys, poly(I:C), or LPS, strongly decreased TAPL transcript, whereas TNF-α, CD40L, and R848 showed only a moderate decrease. Noteworthy is that this down-regulation on mRNA level was not detected on the protein level (data not shown), implying that TAPL has a long half-life.

TAPL Is Not Involved in the Classical MHC Class I Presentation Pathway—Because TAPL is strongly up-regulated in professional antigen-presenting cells, we analyzed its function in the classical pathway of peptide loading of MHC class I molecules in the ER lumen. Two scenarios are conceivable, in which TAPL alone or in complex with TAP1 or TAP2 translocates peptides into the ER lumen. To address this issue, skin fibroblasts derived from bare lymphocyte syndrome type I patients deficient in TAP1 or TAP2 (BRE-169 or STF1-169 cells, respectively) (18, 19, 23) were transfected with human TAPL. TAPL expression was demonstrated by immunoblotting. Conspicuously, TAPL was not detected in non-transfected cells (Fig. 2*A*). Subsequently, MHC I cell surface expression reflecting successful peptide loading of MHC class I molecules in the ER lumen was monitored by flow cytometry using a PE-conjugated anti-HLA-ABC antibody (W6/32) (Fig. 2*B*). TAP-deficient fibroblasts showed a slightly higher fluorescence signal compared with the isotype control, resulting from TAP-independent peptide supply to MHC class I molecules (34, 35). Transfection of TAP1- or TAP2-deficient cells with TAPL did not affect MHC class I surface expression. By contrast, TAP1 or TAP2 restored peptide supply into the ER lumen in cells lacking the corresponding TAP subunit, reflected by an increase in MHC I surface expression. The transfection efficiencies of TAP and TAPL

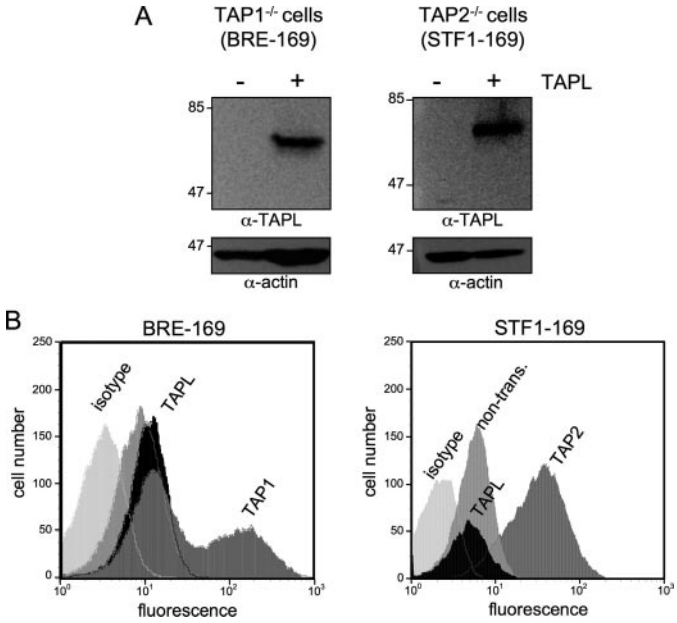

FIGURE 2. **TAPL is not involved in the classical pathway of peptide loading of MHC I molecules in the ER-lumen.** *A*, expression of TAPL in TAP1$^{-/-}$ BRE-169 and TAP2$^{-/-}$ STF1-169 cells. TAP-deficient cells were transiently transfected with pIRES2-TAPL-EGFP. TAPL expression was analyzed by SDS-PAGE and immunoblotting using an epitope-purified anti-TAPL antibody (8). As control, non-transfected cells were analyzed. An equal amount of protein per lane was verified by anti-actin staining. *B*, FACS analysis of MHC class I cell surface expression. For TAPL expression, TAP1-deficient BRE-169 and TAP2-deficient STF1-169 cells were transiently transfected with pIRES2-TAPL-EGFP. TAP1 expression was restored in BRE-169 cells by transient transfection. TAP2 was stably transfected into STF1-169 cells. Cell surface expression of MHC class I was analyzed by flow cytometry using PE-conjugated anti-HLA-ABC and PE-conjugated mouse IgG_2 as an isotype control. Non-transfected cells were used as control.

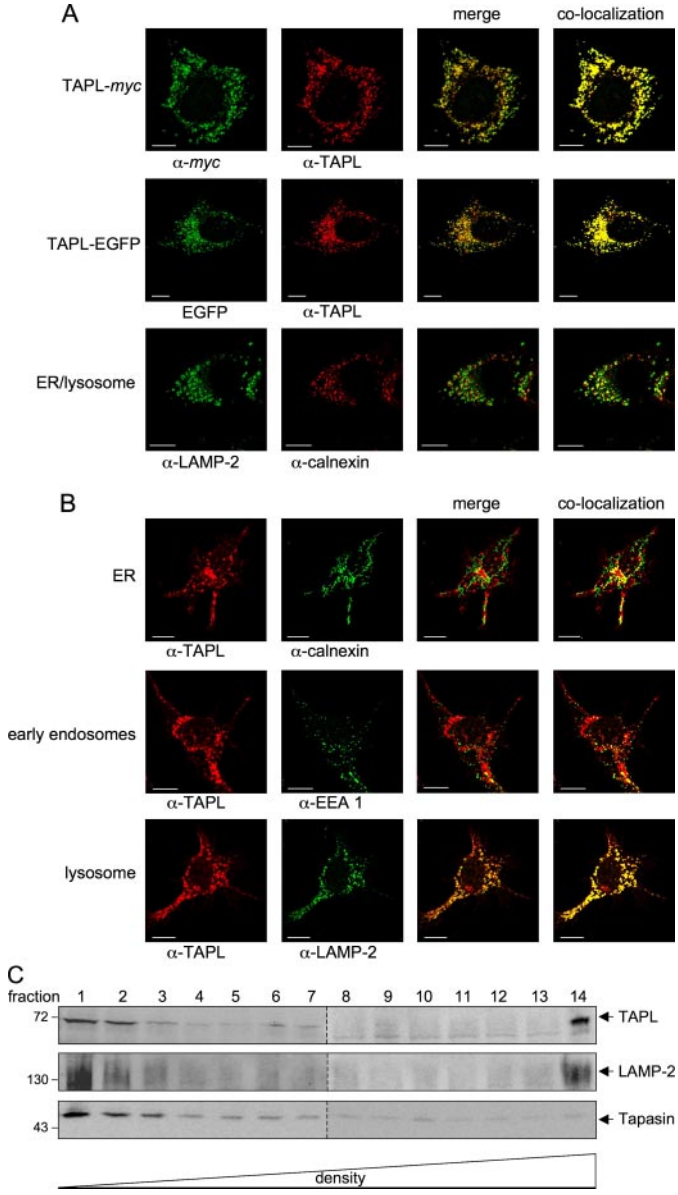

FIGURE 3. **Localization of TAPL in the lysosomal compartment.** *A*, quantitative immunofluorescence microscopy. Confocal images were processed by image restoration and quantitative co-localization. The deconvoluted micrographs as well as their merged images and the merge after co-localization analysis are shown. To demonstrate the quality of the co-localization analysis, HeLa cells were transfected with TAPL-EGFP or TAPL-*myc*. TAPL was detected by EGFP fluorescence or stained with anti-*myc* and/or anti-TAPL antibody. As a negative control, no co-localization was detected with anti-LAMP-2 (*green*) and anti-calnexin antibody (*red*). *B*, co-localization studies of TAPL in stably transduced THP-1 cells. THP-1 cells were stimulated with *E. coli* and grown on lysine-coated coverslips for 48 h. TAPL and subcellular markers (LAMP-2 for lysosomes, EEA1 for early endosomes and calnexin for ER) were stained by specific antibodies and analyzed by quantitative immunofluorescence microscopy. The values for the Pearson correlation are summarized in Table 1. The *scale bar* represents 10 μm. *C*, subcellular fractionation. Non-transduced THP-1 cells were stimulated with *E. coli* for 48 h, and membranes derived from adherent cells were fractioned by a Percoll gradient and analyzed by SDS-PAGE and immunoblotting.

were similar (25%) as monitored by the number of cells with elevated MHC class I level for TAP1 and the co-expression of EGFP for TAPL. In conclusion, TAPL alone or in combination with single TAP subunits does not complement the cellular function of the TAP complex in peptide loading of MHC class I molecules in the ER lumen.

TAPL Is Localized in the Lysosomal Compartment—Because the subcellular localization of TAPL is still under debate (14, 15, 21), we investigated TAPL localization by quantitative immunofluorescence confocal laser-scanning microscopy. To establish the quantification analysis, HeLa cells were transfected with human TAPL containing a C-terminal *myc* tag or EGFP. Two days after transfection, TAPL-*myc* and TAPL-EGFP were detected by immunoblotting as single bands differing by 25 kDa due to the EGFP fusion (supplemental Fig. S1*A*). Notably, intrinsic TAPL expression was not observed in these cells. Both TAPL constructs are functional in peptide transport into intracellular compartments using semi-permeabilized cells (see below).

For quantitative immunofluorescence, cells expressing TAPL-*myc* were stained with anti-*myc* and affinity-purified anti-TAPL antibodies. The deconvoluted micrographs of stained cells, their merged pictures, and the merge after the co-localization analysis are shown in Fig. 3*A*. A co-localization with a Pearson correlation coefficient of 0.73 ± 0.08 was determined (Table 1). A coefficient between zero and −1 indicates no co-localization, whereas a value of 1 attests a perfect co-localization, which can only be reached in theory (36). Similar co-localization coefficients (0.66 ± 0.04) were detected after analysis of TAPL-EGFP with anti-TAPL antibody. As negative control, the double staining of calnexin, an ER-resident protein, and the lysosome-associated membrane protein 2 (LAMP-2) resulted in a Pearson coefficient of 0.04 ± 0.06.

TABLE 1
Pearson correlation of colocalization

Marker 1	Marker 2	Pearson correlation	No. of pictures	Cell line
TAPL-EGFP	TAPL	0.658 ± 0.044 (positive control)	2	HeLa
TAPL-*myc*	TAPL	0.727 ± 0.078 (positive control)	3	HeLa
Calnexin	LAMP-2	0.044 ± 0.058 (negative control)	3	HeLa
TAPL	Calnexin	−0.049 ± 0.082	10	THP-1
TAPL	LAMP-2	0.639 ± 0.089	10	THP-1
TAPL	EEA1	0.075 ± 0.044	8	THP-1
TAPL-EGFP	Calnexin	−0.045 ± 0.038	4	HeLa
TAPL-*myc*	Calnexin	0.084 ± 0.045	4	HeLa
TAPL-EGFP	LAMP-2	0.504 ± 0.129	4	HeLa
TAPL-*myc*	LAMP-2	0.556 ± 0.094	4	HeLa
TAPL-EGFP	EEA1	−0.115 ± 0.105	2	HeLa
TAPL-*myc*	EEA1	−0.04 ± 0.034	2	HeLa

The subcellular localization of TAPL in professional antigen-presenting cells was analyzed in THP-1 cells, a promonocytic cell line widely used as a model system for monocyte to macrophage differentiation. Upon stimulation with LPS or intact *E. coli*, THP-1 cells differentiate into macrophages followed by morphology changes, up-regulation of antigen presentation, and processing elements (37). For immunofluorescence, stably transduced THP-1 cells showing high TAPL expression (supplemental Fig. S2) were stimulated with *E. coli* and stained with anti-TAPL antibody. As shown in Fig. 3*B*, TAPL clearly co-localizes with the lysosomal marker LAMP-2 (Pearson coefficient of 0.639 ± 0.089) but is neither found in the ER (−0.049 ± 0.082) nor in early endosomes (0.075 ± 0.044), as demonstrated by the marker proteins calnexin and early endosome antigen 1 (EEA1), respectively. Similar results and Pearson coefficients were obtained with HeLa cells expressing TAPL-EGFP or TAPL-*myc* (Table 1 and supplemental Fig. S1, *B* and *C*). Based on these data, we conclude that TAPL is exclusively found in the lysosomal compartment, but not in the ER or early endosomes.

To formally rule out that the observed lysosomal localization is due to overexpression of TAPL, we stimulated THP-1 cells with *E. coli* and performed a subcellular fractionation using a Percoll density gradient. Upon stimulation of monocytes to professional antigen-presenting cells, TAPL expression is highly up-regulated (supplemental Fig. S3). Remarkably, TAPL is highly enriched in the dense fraction of the Percoll gradient co-migrating with the lysosomal marker protein LAMP-2 (Fig. 3*C*). Noticeably, this fraction does not contain ER-resident marker proteins, such as tapasin, showing that endogenously expressed TAPL also localizes in lysosomal compartments.

TAPL-specific Peptide Translocation into Lysosomes—After analyzing TAPL in dendritic cells and macrophages, we examined TAPL function in the lysosomal compartment of B-cells. We used human Burkitt's lymphoma (Raji) cells as a model system. After retroviral transduction, TAPL and the Walker A/H-loop mutant K545A/H699A were detected by immunoblotting as single bands (Fig. 4*A*). To uncover TAPL function, lysosomes were purified via Percoll density gradient and peptide translocation was studied using the dense fraction, which is strongly enriched in the lysosomal marker LAMP-2 but deficient in the ER-marker tapasin. Peptide transport is detected

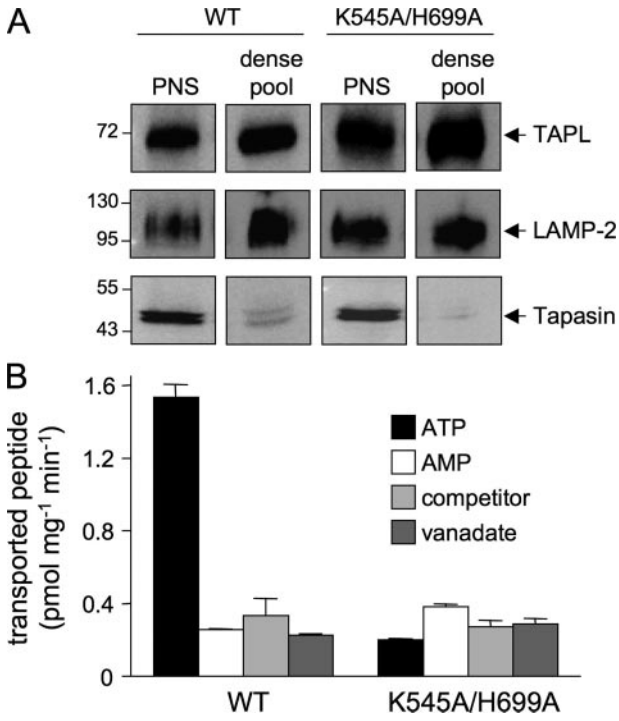

FIGURE 4. **TAPL-specific and ATP-dependent translocation of peptides into lysosomes.** *A*, subcellular fractionation. Perinuclear supernatants (*PNS*) derived from TAPL-wt- or TAPL-K545A/H699A-transduced Raji cells were fractioned by a Percoll gradient and analyzed by SDS-PAGE and immunoblotting. *B*, TAPL-dependent peptide transport into lysosomes. The dense pool of the Percoll gradient was incubated with fluorescein-labeled peptide RRYC(Φ)KSTEL (2 μM) in the presence of ATP or AMP (3 mM) for 30 min at 32 °C. In addition to ATP, 1 mM orthovanadate or 500 μM competitor peptide (RRYQKSTEL) was added to inhibit transport. Transported peptides were quantified by fluorescence (excitation and emission at 485 and 520 nm, respectively). The *y*-axis reflects transported peptide per milligram of lysosomal protein and minute. Data resemble the mean of triplicate measurements.

only in lysosomes containing wild-type (6-fold above background) but not mutant TAPL. Peptide transport is inhibited by orthovanadate, which traps a post-hydrolysis state (38). In addition, the transport is peptide-specific, because it is inhibited by an excess of non-labeled peptide. Similar results were obtained with HeLa cells transiently transfected with TAPL-EGFP or TAPL-*myc*. 3-Fold transport activity above background was observed with saponin semi-permeabilized cells, confirming that the function of TAPL is not affected by the C-terminal tags and is independent of the cell and expression system used. Taken together, we identified a novel ATP-dependent peptide translocation system in lysosomes encoded by the ABC transporter TAPL.

DISCUSSION

For a perfect interplay between different cells mediating the immune response, it is a prerequisite that the antigens are efficiently presented on the surface of professional antigen-presenting cells. TAP-independent access of cytosolic peptides into endolysosomal compartments was reported (5, 7); however, the molecular mechanisms underlying this process are poorly understood. In this study, we demonstrate by using quantitative immunofluorescence and subcellular fractionation that TAPL is found in the lysosomal compartment in professional antigen-presenting cells. TAPL is strongly up-regu-

lated during maturation of peripheral blood monocytes into immature and mature DCs and during differentiation of monocytes to macrophages. We further established an *in vitro* TAPL-dependent peptide translocation assay into isolated lysosomes. Consistent with these results, TAPL was found not to be involved in the classical pathway of MHC I presentation, because it alone or in combination with either TAP1 or TAP2 does not complement TAP function in peptide loading of ER-resident MHC I molecules.

We showed by subcellular fractionation that endogenous and overexpressed TAPL is localized in the dense pool of lysosomes. This result was confirmed by quantitative immunofluorescence microscopy. By image restoration, the background is strongly reduced and co-localization of signals with different intensities can be detected, which is only hardly recognized by conventional overlay. In contrast to previous reports, our data indicate that TAPL is found in lysosomal compartments but not in early endosomes or the ER (14, 21). These results are in agreement with localization studies using stably transfected human ovarian carcinoma cells (15). However, in this previous study, a partial overlap with endosomal staining was visible, which may originate from different cell lines or different markers that have been used for analysis. Because TAP and TAPL are localized in different subcellular compartments, it is not very surprising that no TAPL-TAP heterodimers are formed.

DCs are the most potent antigen-presenting cells and are critical for the initiation of CD4- and CD8-positive T-cell response (39). In the peripheral tissue, immature dendritic cells are specialized in capturing antigens. After stimulation with the appropriate maturation signal, mature dendritic cells migrate to T-cell-rich zones of secondary lymphoid organs and become potent T-cell activators. Interestingly, DCs possess a broad plasticity in response to pathogens and their components, which is reflected in differential gene expression patterns depending on the acquired stimuli (40–42). Stimulation of immature dendritic cells with a mixture composed of TNF-α, IL-1β, IL-6, and prostaglandin E_2 did not significantly change TAPL expression. However, the stimulation of immature dendritic cells by specific factors decreased TAPL expression to different mRNA levels. It is well established that, for example, LPS and TNF-α stimulate the gene expression in immature DCs differentially (43, 44), which is also reflected in a distinct pattern of TAPL expression. LPS seems to initiate the differentiation of the immature to mature DCs. In contrast, the gene expression pattern after treatment with TNF-α resembles more that of untreated cells. Under these conditions, the down-regulation of TAPL is accompanied with the decrease of MHC II transcripts during maturation of DCs in the presence of LPS (43, 44). The high level of TAPL protein in the mature dendritic cells may result from the long half-life of the ABC transporter as it was shown for MHC class II molecules upon treatment of cells with LPS (45).

Professional antigen-presenting cells have the ability of cross-presenting exogenous antigens internalized by pinocytosis or endocytosis on MHC class I molecules by at least two different pathways (for review see Refs. 3, 46). In the TAP-dependent pathway, internalized antigens are delivered to the cytosol where they are processed by the proteasome and subsequently transported by TAP into the ER or phagosomes for loading onto MHC class I (47–49). However, there also exists a TAP-independent pathway, in which exogenous antigens are found in endosomes and degradation products of these antigens are loaded on MHC class I molecules in endolysosomes (50–52).

As a paradigm, MHC class II molecules present exogenously delivered antigens. During cross-presentation, MHC II can stimulate $CD4^+$ T-lymphocyte response to endogenous antigens in tumor and viral infected cells (53–55). Moreover, the delivery of cytoplasmic or nuclear antigens to MHC class II molecules was recently shown (56, 57). This process is dependent on cytoplasmic proteolysis but is clearly TAP-independent (5, 58). Based on the peptide transport system in the lysosomal compartment identified in this study, we hypothesize that TAPL is involved in cross-presentation of cellular or nuclear proteins on MHC class II molecules or in peptide delivery into endolysosomes for presentation of exogenous antigens on MHC I as described above.

In addition, chaperone-mediated autophagy provides a selective mechanism for the delivery and degradation of soluble cytosolic polypeptides in lysosomes (59). In this process, cytosolic proteins are recognized via LAMP-2a and Hsc70 and subsequently translocated into the lumen of the lysosome. It has been reported that this pathway is involved in the presentation of cytosolic autoantigens (60). The transport system within the pathway has nevertheless not been identified so far. It is hard to imagine that the single transmembrane-spanning protein LAMP-2a and the associated chaperone Hsc70 alone can form a translocation complex. We speculate that the lysosomal TAPL membrane translocation system is the key link missing in the chaperone-mediated autophagy and a novel route discharging cytosolic antigens in lysosomal compartments induced in professional antigen-presenting cells.

Acknowledgments—We thank Klaus Hammer, Walter Volknandt, Heinz Schewe, and Bernd Uwe Failer for support in immunocytochemistry and confocal laser scanning microscopy, Randy Teel and Peter Cresswell for retroviral plasmids and help in preparation of lysosomes, and Eckhard Linker and Stefanie Bauer for excellent technical assistance.

REFERENCES

1. Abele, R., and Tampé, R. (2004) *Physiology* (*Bethesda*) **19,** 216–224
2. Pieters, J. (1997) *Curr Opin Immunol* **9,** 89–96
3. Cresswell, P., Ackerman, A. L., Giodini, A., Peaper, D. R., and Wearsch, P. A. (2005) *Immunol. Rev.* **207,** 145–157
4. Malnati, M. S., Marti, M., LaVaute, T., Jaraquemada, D., Biddison, W., DeMars, R., and Long, E. O. (1992) *Nature* **357,** 702–704
5. Dani, A., Chaudhry, A., Mukherjee, P., Rajagopal, D., Bhatia, S., George, A., Bal, V., Rath, S., and Mayor, S. (2004) *J. Cell Sci.* **117,** 4219–4230
6. Day, P. M., Yewdell, J. W., Porgador, A., Germain, R. N., and Bennink, J. R. (1997) *Proc. Natl. Acad. Sci. U. S. A.* **94,** 8064–8069
7. Dissanayake, S. K., Tuera, N., and Ostrand-Rosenberg, S. (2005) *J. Immunol.* **174,** 1811–1819
8. Wolters, J. C., Abele, R., and Tampé, R. (2005) *J. Biol. Chem.* **280,** 23631–23636
9. Koopmann, J. O., Post, M., Neefjes, J. J., Hämmerling, G. J., and Momburg, F. (1996) *Eur. J. Immunol.* **26,** 1720–1728
10. Higgins, C. F. (1992) *Annu. Rev. Cell Biol.* **8,** 67–113

11. Kleijmeer, M. J., Kelly, A., Geuze, H. J., Slot, J. W., Townsend, A., and Trowsdale, J. (1992) *Nature* **357,** 342–344
12. Lacaille, V. G., and Androlewicz, M. J. (1998) *J. Biol. Chem.* **273,** 17386–17390
13. Leveson-Gower, D. B., Michnick, S. W., and Ling, V. (2004) *Biochemistry* **43,** 14257–14264
14. Kobayashi, A., Maeda, T., and Maeda, M. (2004) *Biol. Pharm. Bull.* **27,** 1916–1922
15. Zhang, F., Zhang, W., Liu, L., Fisher, C. L., Hui, D., Childs, S., Dorovini-Zis, K., and Ling, V. (2000) *J. Biol. Chem.* **275,** 23287–23294
16. Kobayashi, A., Hori, S., Suita, N., and Maeda, M. (2003) *Biochem. Biophys. Res. Commun.* **309,** 815–822
17. Uinuk-ool, T. S., Mayer, W. E., Sato, A., Takezaki, N., Benyon, L., Cooper, M. D., and Klein, J. (2003) *Immunogenetics* **55,** 38–48
18. de la Salle, H., Hanau, D., Fricker, D., Urlacher, A., Kelly, A., Salamero, J., Powis, S. H., Donato, L., Bausinger, H., Laforet, M., Jeras, M., Spehner, D., Bieber, T., Falkenrodt, A., Cazenave, J.-P., Trowsdale, J., and Tongio, M.-M. (1994) *Science* **265,** 237–241
19. de la Salle, H., Zimmer, J., Fricker, D., Angenieux, C., Cazenave, J. P., Okubo, M., Maeda, H., Plebani, A., Tongio, M. M., Dormoy, A., and Hanau, D. (1999) *J. Clin. Invest.* **103,** R9–R13
20. Bahram, S., Arnold, D., Bresnahan, M., Strominger, J. L., and Spies, T. (1991) *Proc. Natl. Acad. Sci. U. S. A.* **88,** 10094–10098
21. Kobayashi, A., Kasano, M., Maeda, T., Hori, S., Motojima, K., Suzuki, M., Fujiwara, T., Takahashi, E., Yabe, T., Tanaka, K., Kasahara, M., Yamaguchi, Y., and Maeda, M. (2000) *J. Biochem.* (*Tokyo*) **128,** 711–718
22. Yamaguchi, Y., Kasano, M., Terada, T., Sato, R., and Maeda, M. (1999) *FEBS Lett.* **457,** 231–236
23. Heintke, S., Chen, M., Ritz, U., Lankat-Buttgereit, B., Koch, J., Abele, R., Seliger, B., and Tampé, R. (2003) *FEBS Lett.* **533,** 42–46
24. Gorbulev, S., Abele, R., and Tampé, R. (2001) *Proc. Natl. Acad. Sci. U. S. A.* **98,** 3732–3737
25. Lackman, R. L., and Cresswell, P. (2006) *J. Immunol.* **177,** 4833–4840
26. Jonuleit, H., Kuhn, U., Muller, G., Steinbrink, K., Paragnik, L., Schmitt, E., Knop, J., and Enk, A. H. (1997) *Eur. J. Immunol.* **27,** 3135–3142
27. Brossart, P., Schneider, A., Dill, P., Schammann, T., Grunebach, F., Wirths, S., Kanz, L., Buhring, H. J., and Brugger, W. (2001) *Cancer Res.* **61,** 6846–6850
28. Naviaux, R. K., Costanzi, E., Haas, M., and Verma, I. M. (1996) *J. Virol.* **70,** 5701–5705
29. Radons, J., Faber, V., Buhrmester, H., Volker, W., Horejsi, V., and Hasilik, A. (1992) *Eur J. Cell Biol.* **57,** 184–192
30. Koch, J., Guntrum, R., Heintke, S., Kyritsis, C., and Tampé, R. (2004) *J. Biol. Chem.* **279,** 10142–10147
31. Buelens, C., Verhasselt, V., De Groote, D., Thielemans, K., Goldman, M., and Willems, F. (1997) *Eur. J. Immunol.* **27,** 756–762
32. Brossart, P., Zobywalski, A., Grunebach, F., Behnke, L., Stuhler, G., Reichardt, V. L., Kanz, L., and Brugger, W. (2000) *Cancer Res.* **60,** 4485–4492
33. Wirths, S., Reichert, J., Grunebach, F., and Brossart, P. (2002) *Cancer Res.* **62,** 5065–5068
34. Anderson, K., Cresswell, P., Gammon, M., Hermes, J., Williamson, A., and Zweerink, H. (1991) *J. Exp. Med.* **174,** 489–492
35. Bacik, I., Cox, J. H., Anderson, R., Yewdell, J. W., and Bennink, J. R. (1994) *J. Immunol.* **152,** 381–387
36. Costes, S., Cho, E., Catalfamo, M., Karpova, T., McNally, J., Henkart, P., and Locket, S. (2002) *Proc. Microsc. Microanal.* **8,** 1040–1041
37. Auwerx, J. (1991) *Experientia* **47,** 22–31
38. Sharma, S., and Davidson, A. L. (2000) *J. Bacteriol.* **182,** 6570–6576
39. Mellman, I. (2005) *Adv. Exp. Med. Biol.* **560,** 63–67
40. Mizumoto, N., Hui, F., Edelbaum, D., Weil, M. R., Wren, J. D., Shalhevet, D., Matsue, H., Liu, L., Garner, H. R., and Takashima, A. (2005) *J. Invest. Dermatol.* **124,** 718–724
41. Huang, Q., Liu, D., Majewski, P., Schulte, L. C., Korn, J. M., Young, R. A., Lander, E. S., and Hacohen, N. (2001) *Science* **294,** 870–875
42. Lapointe, R., Toso, J. F., Butts, C., Young, H. A., and Hwu, P. (2000) *Eur. J. Immunol.* **30,** 3291–3298
43. Granucci, F., Vizzardelli, C., Virzi, E., Rescigno, M., and Ricciardi-Castagnoli, P. (2001) *Eur. J. Immunol.* **31,** 2539–2546
44. Efron, P. A., Tsujimoto, H., Bahjat, F. R., Ungaro, R., Debernardis, J., Tannahill, C., Baker, H. V., Edwards, C. K., and Moldawer, L. L. (2005) *J. Endotoxin Res.* **11,** 145–160
45. Wilson, N. S., El-Sukkari, D., and Villadangos, J. A. (2004) *Blood* **103,** 2187–2195
46. Shen, L., and Rock, K. L. (2006) *Curr. Opin. Immunol.* **18,** 85–91
47. Houde, M., Bertholet, S., Gagnon, E., Brunet, S., Goyette, G., Laplante, A., Princiotta, M. F., Thibault, P., Sacks, D., and Desjardins, M. (2003) *Nature* **425,** 402–406
48. Guermonprez, P., Saveanu, L., Kleijmeer, M., Davoust, J., Van Endert, P., and Amigorena, S. (2003) *Nature* **425,** 397–402
49. Ackerman, A. L., Kyritsis, C., Tampe, R., and Cresswell, P. (2003) *Proc. Natl. Acad. Sci. U. S. A.* **100,** 12889–12894
50. Bachmann, M. F., Oxenius, A., Pircher, H., Hengartner, H., Ashton-Richardt, P. A., Tonegawa, S., and Zinkernagel, R. M. (1995) *Eur. J. Immunol.* **25,** 1739–1743
51. Norbury, C. C., Princiotta, M. F., Bacik, I., Brutkiewicz, R. R., Wood, P., Elliott, T., Bennink, J. R., and Yewdell, J. W. (2001) *J. Immunol.* **166,** 4355–4362
52. Lizee, G., Basha, G., Tiong, J., Julien, J. P., Tian, M., Biron, K. E., and Jefferies, W. A. (2003) *Nat. Immunol.* **4,** 1065–1073
53. Jaraquemada, D., Marti, M., and Long, E. O. (1990) *J. Exp. Med.* **172,** 947–954
54. Jacobson, S., Sekaly, R. P., Jacobson, C. L., McFarland, H. F., and Long, E. O. (1989) *J. Virol.* **63,** 1756–1762
55. Wang, R. F., Wang, X., Atwood, A. C., Topalian, S. L., and Rosenberg, S. A. (1999) *Science* **284,** 1351–1354
56. Chicz, R. M., Urban, R. G., Gorga, J. C., Vignali, D. A., Lane, W. S., and Strominger, J. L. (1993) *J. Exp. Med.* **178,** 27–47
57. Rudensky, A., Preston-Hurlburt, P., Hong, S. C., Barlow, A., and Janeway, C. A., Jr. (1991) *Nature* **353,** 622–627
58. Lich, J. D., Elliott, J. F., and Blum, J. S. (2000) *J. Exp. Med.* **191,** 1513–1524
59. Majeski, A. E., and Dice, J. F. (2004) *Int. J. Biochem. Cell Biol.* **36,** 2435–2444
60. Zhou, D., Li, P., Lin, Y., Lott, J. M., Hislop, A. D., Canaday, D. H., Brutkiewicz, R. R., and Blum, J. S. (2005) *Immunity* **22,** 571–581